Vol. 83 (1993) *ACTA PHYSICA POLONICA A* No. 6

INFRARED-TO-VISIBLE UPCONVERSION IN ERBIUM PENTAPHOSPHATE*

F. Kaczmarek, M. Balicki and J. Karolczak

Quantum Electronics Laboratory, Institute of Physics, A. Mickiewicz University
Grunwaldzka 6, 60-780 Poznań, Poland

(Received March 5, 1993; in final form April 13, 1993)

Infrared-to-visible upconversion has been observed by many authors in a variety of rare-earth-doped crystals. This paper reports the study of the upconversion found in stoichiometric erbium pentaphosphate, ErP_5O_{14}. Strong green fluorescence was observed upon pumping the crystal with a cw diode laser at a wavelength of about 800 nm.

PACS numbers: 78.55.–m, 78.55.Hx

1. Introduction

Efficient infrared-to-visible upconversion in rare-earth compounds was first observed as early as in 1969 by Johnson and Gugenheim [1], and also by Van Uitert et al. [2]. Two-, three-, and four-photon processes were found responsible for blue, green, or red fluorescence when doped crystals (e.g. $BaLuF_5$:5% Yb^{3+}, 3% Ho^{3+} or Y_3OCl_7:Yb^{3+}, Er^{3+}) were irradiated with the emission of an Si-doped GaAs luminescent diode operating at a wavelength of about 930 nm. The green fluorescence centered at 550 nm varies as square of the infrared pump power and arises from two successive energy transfers from Yb^{3+} to Ho^{3+} ions. Infrared-pumped visible lasers (operating at liquid nitrogen temperature) in Yb^{3+}- or Er^{3+}-doped crystals were demonstrated by Johnson and Gugenheim [3] and Silversmith et al. [4]. The rare-earth-doped compounds contained a few percent of Yb^{3+} or Er^{3+} ions.

We wish to report on strong green fluorescence in stoichiometric erbium pentaphosphate, ErP_5O_{14}, when pumped by a cw diode laser whose broad band emission was centered at 800 nm. The concentration of active Er^{3+} ions was $3.78 \times 10^{21}/cm^3$.

The pentaphosphate ribbon-like crystal structure efficiently isolates active ions which accounts for the fact that quenching of the fluorescence is relatively

---

*This work was supported by the Committee for Scientific Research grant no. 2P 30202704.

weak and permits laser emission even at room temperatures. Laser operation in a variety of rare-earth pentaphosphates and also in rare-earth tetraphosphates have been observed by many authors (e.g. [5–9]). We expected that the upconversion process would be strong enough to yield visible fluorescence that could lead to laser emission at sufficiently high pumping power.

2. Experimental

ErP_5O_{14} monocrystals were grown according to the method previously described in [10]. Small ErP_5O_{14} platelets, 0.2–0.5 mm in thickness, and up to 5 mm in diameter were used. The crystal structure of ErP_5O_{14} determined by Jeżowska-Trzebiatowska et al. [11] is monoclinic of the space group $C_{2/c}$, with $a = 12.837$ Å, $b = 12.723$ Å, $c = 12.381$ Å and $\beta = 91.25°$. A single cell contains 8 ErP_5O_{14} molecules. The shortest Er^{3+}–Er^{3+} distance found was 5.70 Å. The density and the refractive index of our crystals were measured to be: $\rho = 3.64 \pm 0.001$ g/cm^3, and n (along the c-axis) $= 1.71 \pm 0.02$ (at $\lambda = 632.8$ nm). The accuracy of the n-measurement was limited by the Brewster method applied. The number of active ions per cm^3 amounted to 3.78×10^{21}.

We were interested mainly in observing the process of upconversion, nevertheless the absorption and fluorescence spectra were also determined. Absorption bands and their peak values are summarized in Table (from 26800–6600 cm^{-1}). The table also includes numerical values characterizing the transitions observed. For the sake of comparison, free-ion transitions, and those in a 0.5% Er^{3+}-doped glass were given (after Rajniak [12] and Shinn et al. [13]). The calculated and measured oscillator strengths for Er^{3+}-doped glass (also after [12] and [13]) are also listed. Since the oscillator strength is directly related to absorption, it was interesting to compare our α_p-values with the oscillator strengths calculated and measured for Er^{3+} glass. We chose arbitrarily the ${}^4G_{11/2}$ line as the reference one, and analyzed the display of the relative α_p, f_r^t, and f_r^m ratios. As seen from Table, the coincidence between the transition frequencies for free ions and for the Er^{3+} ions in ErP_5O_{14} crystal is remarkable. On the other hand, the relative α_p^*, f_r^t, and f_r^m values exhibit quite large differencies, with a few exceptions. Unfortunately, absorption at the pumping frequency to the ${}^4I_{9/2}$ level ($\alpha = 2.6$ cm^{-1}) as well as the oscillator strength of this transition in Er^{3+}-doped glass are small. The complex absorption line shape at the pumping frequency does not permit precise determination of the oscillator strength, f. Using the following formula [14]:

$$f = \frac{mc^2}{\pi N e^2} \chi \int \alpha(\tilde{\nu}) d\tilde{\nu},$$

where $\tilde{\nu}$ is expressed im cm^{-1}, m and e are the electron mass and charge, respectively, N is the number of Er^{3+} ions in cm^3, and $\chi = 9n/(n^2+2)^2$ is a correction factor for the refractive index of the medium, we obtained an approximate value $f = 28 \times 10^{-8}$ which is very close to the experimental f-value found for Er^{3+}-doped glass.

It is assumed [3, 4] that in the ion–pair cooperative process, the second ion in the pair transfers its energy to the first one which, in turn, undergoes excitation to higher energy levels, and — later on — emits anti-Stokes radiation (see Fig. 1).

TABLE

Numerical values characterizing the absorption transitions in ErP_5O_{14} at room temperature. For the sake of comparison, transitions in free-ion and in Er^{3+}-doped glass are also listed (after [12], [15] and [16]). α_p and σ_p denote peak values; $\tilde{\nu}_g(\tilde{\nu}_f)$ — transition wavenumbers found in erbium doped glass and in free ions, respectively; f^t — calculated oscillator strength in glass [13]; f^m — measured oscilator strength in glass [13]; α_p^* — $\alpha_p/\alpha_p(^4G_{11/2})$; f_r^t — $f^t/f^t(^4G_{11/2})$; f_r^m — $f^m/f^m(^4G_{11/2})$.

LSJ designation	Spectral band [cm^{-1}]	Peak values [cm^{-1}]	α_p [cm^{-1}]	σ_p [cm^2] $\times 10^{21}$	$\tilde{\nu}_g$ ($\tilde{\nu}_f$)	f^t $\times 10^8$	f^m $\times 10^8$	α_p^*	f_r^t	f_r^m
$^4G_{11/2}$	28000–26000	26500	73.65	19.50	26455 (26262)	740.4	841	1.000	1.000	1.000
		26340	78.49	20.70						
		26140	15.99	4.23						
$^2H_{9/2}$	24800–24300	24640	8.22	2.17	24630 (24457)	62.2	41	0.110	0.079	0.048
		24580	6.76	1.78						
$^4F_{3/2}$	22700–22500	22620	3.62	0.95	– (22407)	68.4	–	0.050	0.087	–
		22560	4.70	1.24						
$^4F_{5/2}$	22450–22000	22400	1.85	0.48	– (22066)	68.4	71	0.115	0.087	0.084
		22220	8.46	2.24						
		22020	4.48	1.18						
$^4F_{7/2}$	20700–20300	20520	23.40	6.19	20534 (20406)	153.0	141	0.317	0.196	0.167
		20320	11.91	3.15						
$^2H_{11/2}$	19400–18800	19240	39.67	10.50	19194 (19035)	432.0	394	0.490	0.550	0.460
		19180	36.48	9.65						
		19100	37.09	9.81						
		18900	11.37	3.00						
$^4S_{3/2}$	18600–18200	18500	5.14	1.36	18450 (18290)	37.4	39	0.115	0.047	0.046
		18400	8.47	2.24						
		18220	2.57	0.68						
$^4F_{9/2}$	15500–14900	15340	20.62	5.45	15314 (15174)	173.7	164	0.280	0.220	0.190
		15200	4.59	1.21						
		15020	7.24	1.91						
$^4I_{9/2}$ (pump.)	12700–12300	12480	2.57	0.67	12500 (12350)	23.9	20	0.035	0.030	0.024
		12350	0.86	0.22						
$^4I_{11/2}$	10400–10200	10300	13.05	3.45	10245 (10110)	42.2	56	0.120	0.054	0.066
		10250	8.71	2.30						
$^4I_{13/2}$	–	–	–	–	6596 (6481)	97.6	46	–	0.130	0.054

We performed further pumping experiments using a dye laser, and, first of all, a diode laser, temperature-tuned to the absorption transition $^4I_{15/2} \Rightarrow {}^4I_{9/2}$. Fluorescence in the green for diode laser pumping at room temperature and at liquid nitrogen temperature is shown in Fig. 2. Fluorescence intensity at $\lambda \approx$ 550 nm increased 3.7 times upon lowering the temperature to 77 K.

The dye laser excites the Er^{3+} ions directly to the energy levels above the initial fluorescence level ($^4S_{3/2}$). On the other hand, the infrared laser excites the

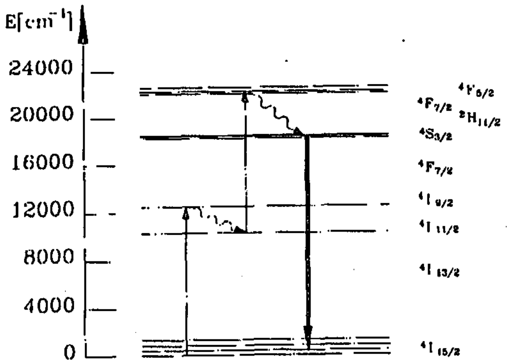

Fig. 1. Illustration of the upconversion process.

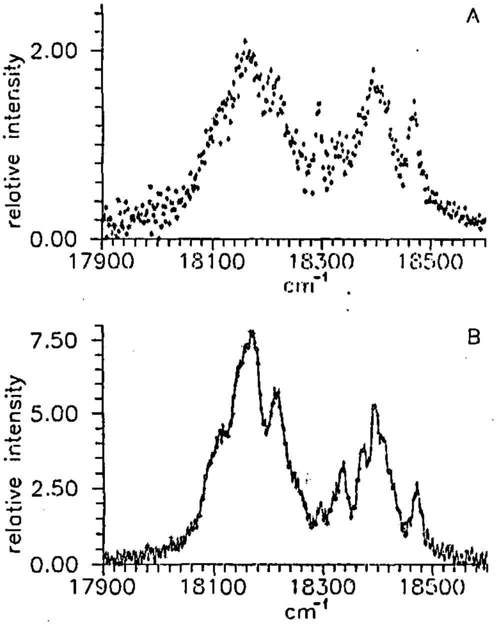

Fig. 2. Fluorescence in the green of ErP_5O_{14}: (a) excitation source — cw diode laser, $\lambda \approx 800$ nm, room temperature, pumping power ≈ 300 mW; (b) as in (a), but at liquid nitrogen temperature.

$^4I_{9/2}$ level, well below the fluorescent one, indicating the role of the cooperative process. In the first stage of our experiments the diode laser emitted up to 500 mW of infrared power.

Directional strong green fluorescence was intensive enough to be observed not only perpendicularly to the pumping beam (see Fig. 3), but also on a white screen

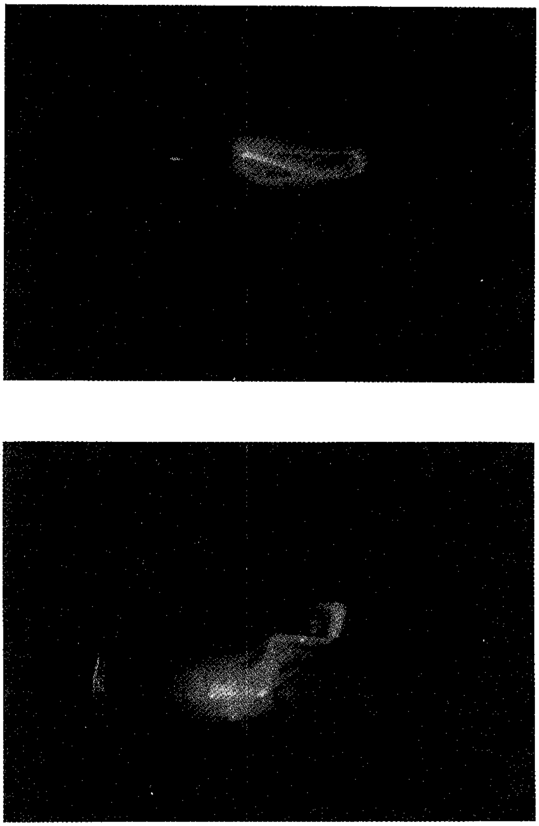

Fig. 3. Infrared-to-visible upconversion in two small ErP_5O_{14} crystals (active length of about 4–5 mm). Due to total internal reflection of the exciting beam, the green fluorescence follows the path of the infrared beam.

behind the crystal. The broad band emission consisted of distinctly resolved four main lines with $\lambda = 550.42$ nm, 543.54 nm, 543.12 nm, and 541.42 nm. The overall emission band spans from 18540 cm^{-1} ($\lambda \approx 540$ nm) to 17980 cm^{-1} ($\lambda = 556$ nm). The main fluorescence line of a wave number of 18398 cm^{-1} ($\lambda = 543.54$ nm) is practically not absorbed in the crystal, since the nearest absorption line at 12260 cm^{-1} is characterized by an absorption coefficient of 2.6 cm^{-1}. However, attempts to obtain laser operation for a sample placed within a high-Q optical resonator proved unsuccessful. Further experiments, using more powerful diode laser and a special chamber (the crystal will be kept in vacuum at liquid nitrogen temperature) are now in progress.

This work proves that infrared-to-visible upconversion process in stoichiometric rare-earth crystal is possible due to the specific crystal structure which makes fluorescence quenching weak, even at active ion concentrations of order of 10^{21} cm^{-3}.

References

[1] L.F. Johnson, H.J. Gugenheim, *Appl. Phys. Lett.* **15**, 51 (1969).

[2] L.G. Van Uitert, S. Singh, H.J. Levinstein, L.F. Johnson, W.H. Grodkiewicz, J.E. Geusic, *Appl. Phys. Lett.* **15**, 53 (1969).

[3] L.F. Johnson, H.J. Gugenheim, *Appl. Phys. Lett.* **19**, 44 (1971).

[4] A.J. Silversmith, W. Lenth, R.M. Macfarlance, *Appl. Phys. Lett.* **51**, 1977 (1987).

[5] H.G. Danielmeyer, H.P. Weber, *IEEE J. Quantum Electron.* **8**, 805 (1972).

[6] G. Huber, W.W. Krühler, W. Bludau, H.G. Danielmeyer, *J. Appl. Phys.* **46**, 3580 (1975).

[7] H.P. Weber, P.F. Liao, B.C. Tofield, *IEEE J. Quantum Electron.* **10**, 563 (1974).

[8] F. Kaczmarek, M. Szymański, *Appl. Phys.* **13**, 55 (1977).

[9] M. Szymański, J. Karolczak, F. Kaczmarek, *Appl. Phys.* **19**, 345 (1979).

[10] B. Borkowski, E. Grzesiak, F. Kaczmarek, Z. Kałuski, J. Karolczak, M. Szymański, *J. Cryst. Growth* **44**, 320 (1978).

[11] B. Jeżowska-Trzebiatowska, Z. Mazurek, T. Lis, *Acta Crystallogr. B* **36**, 1639 (1980).

[12] K. Rajniak, *J. Chem. Phys.* **43**, 847 (1965).

[13] M.D. Shinn, W.A. Sibley, M.G. Drexhage, R.N. Brown, *Phys. Rev. B* **27**, 6635 (1983).

[14] W.T. Carnall, P.R. Fields, B.G. Wybourne, *J. Chem Phys.* **42**, 3797 (1965).

[15] W.F. Krupke, J.B. Gruber, *J. Chem. Phys.* **41**, 1225 (1964).

[16] M.J. Weber, *Phys. Rev.* **156**, 231 (1967).